Proc. Natl. Acad. Sci. USA
Vol. 94, pp. 5078–5083, May 1997
Cell Biology

Microtubule release from the centrosome

T. J. KEATING*, J. G. PELOQUIN, V. I. RODIONOV, D. MOMCILOVIC, AND G. G. BORISY

Laboratory of Molecular Biology, University of Wisconsin, Madison, WI 53706

Communicated by S. J. Peloquin, University of Wisconsin, Madison, WI, February 18, 1997 (received for review January 12, 1997)

ABSTRACT **Although microtubules (MTs) are generally thought to originate at the centrosome, a number of cell types have significant populations of MTs with no apparent centrosomal connection. The origin of these noncentrosomal MTs has been unclear. We applied kinetic analysis of MT formation *in vivo* to establish their mode of origin. Time-lapse fluorescence microscopy demonstrated that noncentrosomal MTs in cultured epithelial cells arise primarily by constitutive nucleation at, and release from, the centrosome. After release, MTs moved away from the centrosome and tended to depolymerize. Laser-marking experiments demonstrated that released MTs moved individually with their plus ends leading, suggesting that they were transported by minus end-directed motors. Released MTs were dynamic. The laser marking experiments demonstrated that plus ends of released MTs grew, paused, or shortened while the minus ends were stable or shortened. Microtubule release may serve two kinds of cellular function. Release and transport could generate the noncentrosomal MT arrays observed in epithelial cells, neurons, and other asymmetric, differentiated cells. Release would also contribute to polymer turnover by exposing MT minus ends, thereby providing additional sites for loss of subunits. The noncentrosomal population of MTs may reflect a steady-state of centrosomal nucleation, release, and dynamics.**

The centrosome, consisting of two centrioles surrounded by an amorphous cloud of pericentriolar material, is thought to be the primary site of nucleation for cytoplasmic microtubules (MTs) in animal cells. Nonetheless, a number of cell types contain significant proportions of noncentrosomal MTs (for review, see ref. 1). Several mammalian cell types, including neurons (2) and skeletal muscle cells (3) as well as epithelial cells from liver (4), kidney (5), intestine (6), and cochlea (7), have large arrays of noncentrosomal MTs that are important for the cells' specialized functions. In polarized epithelial cells in particular, MTs run in parallel arrays, with the minus ends at the apical surface and the plus ends at the basal surface (8), an arrangement that supports polarized sorting of membrane components and vesicle traffic (6). Although the centrosome is in the apical region, the MT minus ends are not evidently associated with the centrosome but terminate along the apical surface.

A priori, four classes of mechanism could generate noncentrosomal MTs: self-assembly of MTs in the cytoplasm, nucleation of MTs at noncentrosomal sites, breakage or severing of centrosomal MTs along their length, and release of MTs from the centrosome. Work performed in a variety of systems has provided indirect evidence for release of MTs from the centrosome. In sea urchin eggs (9, 10) and Dictyostelium cells (11), reorganization of the interphase MT array into the mitotic spindle is preceded by what appears to be release of nearly all of the MTs from the centrosome or spindle pole body, respectively. In epithelial cells during regrowth of the interphase MT array after complete depolymerization, MTs are initially found only at the centrosome but at later times become noncentrosomally located (12–14), suggesting that MTs are first nucleated at the centrosome and are then translocated to other regions of the cell. In neurons, several lines of evidence indicate that axonal MTs arise from released centrosomal MTs (15–17). Nonetheless, the results discussed above all have been obtained from populations of cells fixed at relatively infrequent time points, with the phenomenon of MT release being inferred from static images.

Additional evidence comes from analysis of cytosolic extracts produced from *Xenopus* eggs. Belmont *et al.* (18) saw release of MTs from the centrosome, as well as movement of MT segments across the coverslip, in both interphase and mitotic extracts. It could not be excluded, however, that the release observed was an *in vitro* artifact, perhaps resulting from an excess of minus end-directed motors adsorbed onto the coverslip surface and pulling on the MTs.

The existence in interphase cells of significant numbers of noncentrosomal MTs with free minus ends suggests a need for a rethinking of mechanisms of MT turnover *in vivo*. MT assembly nucleated by interphase centrosomes *in vitro* is characterized by phases of MT plus end growth and shortening back to the centrosome, termed "dynamic instability," with minus ends of MTs stably anchored to the centrosome (19). Dynamic instability is also the predominant mechanism of MT turnover observed *in vivo* at the periphery of cells (20, 21). However, in interphase cells, shortening MTs are frequently rescued, resulting in only minor excursions of depolymerization (22). Yet reported rates of exchange of tubulin dimers with polymer indicate a rapid turnover of the MT array (23). Moreover, a computer simulation of MT dynamic instability using measured assembly parameters of MT plus ends indicates MT turnover would be very slow (24). This disparity between the behavior of individual MT plus ends and the turnover of populations of MTs suggests that plus end dynamic instability does not adequately describe MT turnover *in vivo*. Indeed, plus ends are not the only possible sites of MT disassembly. A treadmilling mechanism in which minus ends are the primary site of depolymerization was established by biochemical experiments for MTs *in vitro* (25). Recently, we showed in cytoplasmic fragments from melanophores that free MTs exhibited treadmilling behavior (26). Also, in mitotic spindles, continuous disassembly of kinetochore MTs occurs at their minus ends and makes a substantial contribution to kinetochore MT turnover (27, 28). We report here results from direct observation of MT behavior at the centrosome *in vivo* that have significance for our understanding of the origin of noncentrosomal MT arrays and MT turnover.

MATERIALS AND METHODS

Cell Culture. PtK_1 rat kangaroo kidney epithelial cells (American Type Culture Collection) were cultured in F-10

The publication costs of this article were defrayed in part by page charge payment. This article must therefore be hereby marked "*advertisement*" in accordance with 18 U.S.C. §1734 solely to indicate this fact.

0027-8424/97/945078-6$2.00/0
PNAS is available online at **http://www.pnas.org**.

Abbreviation: MT, microtubule.

*To whom reprint requests should be addressed. e-mail: tkeating@facstaff.wisc.edu.

media (GIBCO) supplemented with 10% fetal bovine serum (HyClone), 20 mM Hepes, and antibiotics and kept at 37°C. Two to four days before experiments, cells were plated into observation chambers made by attaching a coverslip with Sylgard silicone elastomer (Dow–Corning) over a hole drilled in a 35-mm culture dish.

Preparation of Cy3-Tubulin. Microtubule protein was prepared from porcine brain by cycles of assembly and disassembly (29). Tubulin depleted of microtubule-associated proteins was obtained by assembly in 0.5 M Pipes, 5 mM $MgCl_2$, and 1 mM GTP (pH 6.9) containing 10% dimethyl sulfoxide (30). The MTs were sedimented at 200,000 × *g* at 37°C for 5 min in a TLS-55 rotor (Beckman). The supernatant containing microtubule-associated protein was aspirated, and the MT pellet was resuspended in two pellet volumes of 0.1 M PIPES/1 mM $MgCl_2$, pH 6.9 (PM) containing 10% dimethyl sulfoxide at 37°C. One vial (≈0.2 mg) of Cy3 reactive dye (Research Organics) dissolved in 20 μl of anhydrous dimethyl sulfoxide was added for each 4 mg of tubulin, and the reaction was incubated at 37°C for 30 min. The labeled MTs were sedimented (200,000 × *g* at 37°C for 10 min in a TLS-55 rotor) through a 33% glycerol cushion in PM, resuspended in five pellet volumes of cold PM, and depolymerized by incubating at 0°C for 10 min. The tubulin solution was sedimented at 200,000 × *g* at 4°C for 5 min in a TLA-100 rotor (Beckman). The soluble tubulin was polymerized with 10% dimethyl sulfoxide and 1 mM GTP at 37°C for 10 min. The MTs were sedimented through a glycerol cushion again, and the depolymerization and cold spin were repeated. The labeled tubulin was frozen in 10-μl aliquots in liquid nitrogen. The reaction gave a yield of 30–50% and a labeling stoichiometry of 0.5 Cy3 molecules per tubulin dimer based on an absorption coefficient of 150,000 $M^{-1}\cdot cm^{-1}$ for Cy3 (31). Protein concentration was measured by bicinchoninic acid protein assay (Pierce). Before microinjection, a 10-μl aliquot of Cy3–tubulin was centrifuged at 200,000 × *g* for 10 min at 4°C to remove particulate material and to reduce pipette clogging and was stored on ice until the time of injection.

Imaging and Data Analysis. Cells injected with Cy3–tubulin were treated with the oxygen-depleting agent Oxyrase (Oxyrase, Ashland, OH) to reduce photodamage and photobleaching (32). At least 30 min before observation, Oxyrase was added to the observation chamber at a final dilution of 2% (vol/vol) of the original stock, along with lactic acid at a final concentration of 20 mM. The Oxyrase-treated dishes were then covered with a layer of mineral oil (Squibb) to retard gas exchange, keeping O_2 out of the chamber and CO_2 in.

Injected cells were observed on a Nikon Diaphot 300 inverted microscope equipped with a Plan ×100, 1.25 NA objective. Images were collected with a slow scan, cooled CCD camera (CH250; Photometrics, Tucson, AZ) driven by METAMORPH imaging software (Universal Imaging, Media, PA). The image of microtubule fluorescence was projected onto the CCD chip with a magnification of 0.1 μm/pixel. Exposure times were 0.25–0.5 s, and images were collected at 4- to 6-s intervals. Cells were kept at 37°C during observation.

Laser bleaching (20) of Cy3-labeled MTs was performed with the 514-nm line of a 3 W Argon-ion laser (Spectra-Physics) with power levels ranging from 100 to 500 mW and pulse durations of 20–220 msec. In cases in which the plus ends of MTs were bleached, the ends subsequently grew, demonstrating that laser bleaching did not damage the MTs themselves. Laser bleaching experiments were performed at 22°C.

Images were processed with METAMORPH and PHOTOSHOP (Adobe Systems, Mountain View, CA) to reduce out-of-focus haze and to enhance contrast of MTs. To highlight the MT of interest in each figure, a red overlay was painted over the MT in PHOTOSHOP with opacity set to 25%. Because of the difficulty in seeing the exact termination point of the MT at the centrosome, positions of overlays at the minus ends of centrosomal MTs are only approximate.

RESULTS

Visualization of Single Microtubules Near the Centrosome in Living Cells. Previous studies of MT behavior in living cells have concentrated on peripheral regions where MTs are sparse and background fluorescence is low (20–22). It is more difficult to distinguish single MTs in central regions of the cell because of numerous overlapping MTs and high levels of background fluorescence arising from labeled tubulin monomers and out-of-focus MT polymer. We developed an observation protocol taking advantage of cellular geometry that enabled us to see individual MTs at the centrosome. We chose cells that were flat and well spread, further selecting for cells in which the centrosome was at the ventral (coverslip) surface and focusing our observations on the region of cytoplasm between the coverslip and nucleus (Fig. 1). In this region, MTs were constrained to a single focal plane, permitting them to be followed for appreciable lengths. Under these conditions, MT activity at the centrosome was directly observed.

An additional approach that facilitated single-MT resolution was to observe MTs shortly after injection of fluorescent tubulin but before complete equilibration of the labeled subunits. During the first 10–15 min after fluorescent tubulin injection, a smaller proportion of MTs near the centrosome contained fluorescent subunits than at equilibrium (as expected for tempered dynamic instability; see ref. 33), making individual MTs much easier to follow. Nevertheless, although this approach facilitated single MT observation, it was not absolutely necessary to use this technique to see MT release. MT release also was observed after steady-state labeling.

Microtubules Are Released from the Centrosome. Using the techniques described above, we collected time-lapse sequences focused on the centrosome of Cy3-labeled MTs in interphase PtK_1 cells. A typical sequence consisted of 150 images acquired

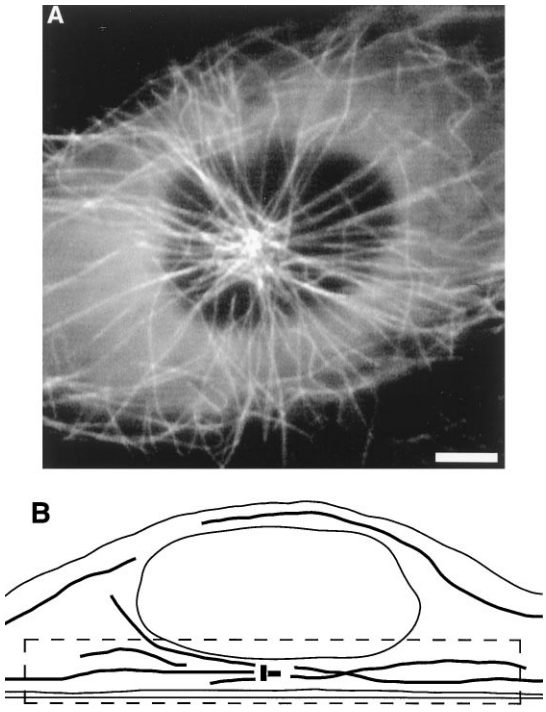

FIG. 1. Fluorescently labeled MTs in PtK_1 cells. (*A*) Fluorescent MTs in a living PtK_1 cell. The nucleus excludes MTs and tubulin monomers, creating a region in the center of the cell with little or no background fluorescence. In the cell shown here, the centrosome is in the center of this darkened region, making it easier to see single MTs. (Bar = 5 μm.) (*B*) Diagram depicting the geometrical relationship among the ventral cortex, the centrosome, MTs, and the nucleus as seen in side view; the components are not necessarily drawn to scale. The dashed lines show the approximate region of focus.

4 s apart, thus spanning 10 min. The observation window of 10 min was initiated as early as 2 min or as late as 60 min after injection of labeled tubulin. Over the course of the experiments, 67 cells and ≈1700 MTs were analyzed. In every cell examined, MT release from the centrosome was observed (Fig. 2). Because of geometrical limitations, MTs could not be analyzed for a full 360° about each centrosome; rather MTs were analyzed within defined sectors. Normalizing the rate of release (average = 1.5 min^{-1}; range = 1–3 min^{-1}) to the number of centrosomal MTs in the sector examined (average = 25; range = 10–55), ≈6% of the centrosomal MTs was released per minute. Most of the release events observed were in the nuclear–ventral region of cytoplasm, mainly because this is where it was easiest to see single MTs. Nonetheless, a number of MTs that were not located in the nuclear–ventral region also were seen to be released and transported through the cytoplasm (not shown).

Depending on the density of MTs at the centrosome, it was often possible to observe nucleation of new MTs (Fig. 2*A*). Some of these MTs were subsequently released. The fact that we could see both nucleation and release of the same MT demonstrates that released MTs were initially attached to the centrosome rather than simply residing next to it.

The observation of release necessarily requires that the MT minus end be displaced from the centrosome. After release, most MTs moved away from the centrosome in a radial trajectory. The MTs either buckled (Fig. 2, *A* and *C*) or remained straight (Fig. 2*B*), the leading end either advanced (Fig. 2*A*) or stopped (Fig. 2, *B* and *C*), and the MT length either remained almost constant (Fig. 2*A*, 89–105 s) or

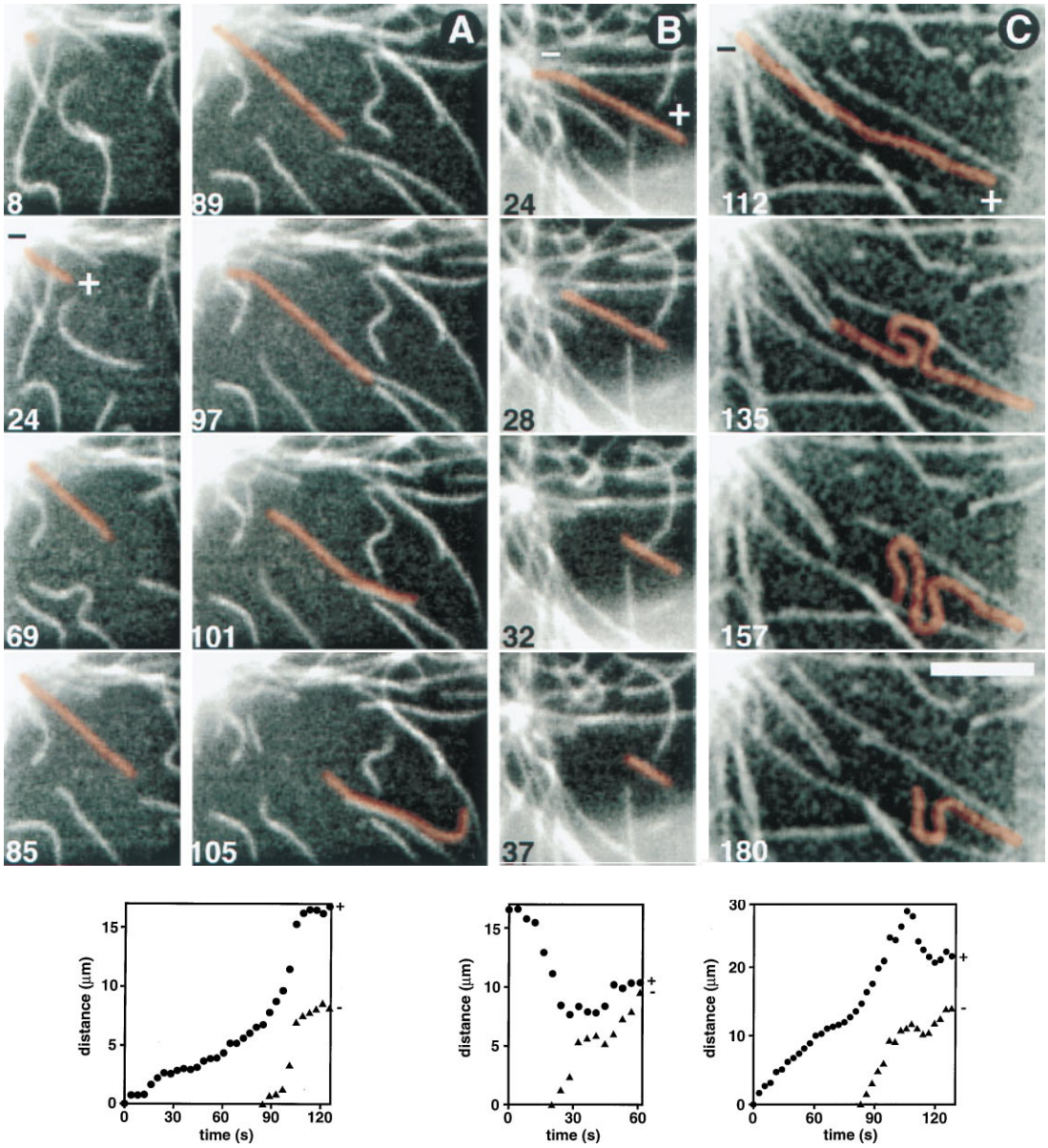

FIG. 2. Microtubule nucleation and release from the centrosome. In all three examples, the centrosome is in the upper left corner of the frame and the MT traverses the nuclear–ventral zone. Time (seconds) at which the image was collected is shown in the lower left corner of each frame. The MT of interest is highlighted by a semitransparent red overlay. Minus and plus ends of the MT are labeled − and +, respectively. Graphs below each sequence show the distance of the MT plus (+, circles) and minus (−, triangles) ends from the centrosome vs. time. Vertical dotted lines indicate the times at which the frames were acquired. The distance of the plus end from the centrosome was measured along the contour of the MT. (*A*) MT is shown shortly after its nucleation at the centrosome until after its release (between 85 and 89 s) and movement across the nuclear–ventral region (>89 s). The plus end of the MT bends (105 s). (*B*) MT is released, and the minus end moves away from centrosome while the plus end remains in the same position. (*C*) MT is released and moves away from the centrosome. The MT buckles (135 s) and begins to shorten, presumably from its minus end. (Bar = 5 μm.)

decreased (Fig. 2, *B* and *C*). Movement of the minus end away from the centrosome could occur either by motor-based translocation or by loss of subunits from the minus end. The extensive buckling of MTs seen in some cases (Fig. 2*C*) suggests a motor-based mechanism; the extensive shortening seen in some cases (Fig. 2*B*) suggests minus end depolymerization. Both processes may occur on the same MT (Fig. 2*C*). Finally, for some MTs, both the plus and minus ends moved away from the centrosome at nearly equivalent rates (Fig. 2*A*), which could be produced either by motor-based transport or by treadmilling (25, 26).

Analysis of Laser-Marked Microtubules. To determine which mechanisms were producing the observed MT movements, a reference mark was placed on the MTs by fluorescence photobleaching (Fig. 3). Movement of the mark relative to the centrosome would signify MT transport. Alternatively, if the mark remained stationary relative to the centrosome but the distance between the mark and the minus end decreased, depolymerization from the minus end would be indicated. Plus end growth coupled with minus end shortening would appear as movement but in fact would be treadmilling. An excess of minus end shortening over plus end growth would appear as movement, but the MT would become progressively shorter and ultimately disappear. Time-lapse imaging of marked MTs revealed that both minus end shortening as well as translocation of whole MTs contributed to movement of MT minus ends away from the centrosome (Fig. 3). Both the plus and minus ends of released MTs were dynamic, the plus end exhibiting phases of growth, shortening, and pause and the minus end only staying stable or shortening (Fig. 3). In a few cases, minus end shortening coincided with a period of plus end growth, producing treadmilling (Fig. 3*B*). The movements of released MTs were generally complex, as illustrated by the fact that the treadmilling behavior shown in Fig. 3*B* is occurring on a MT that also is being transported.

Motor-based movement of MTs, assayed by movement of the reference mark, was erratic, with the rate varying considerably even for a single MT (Fig. 3*A*). As was suggested by Belmont *et al.* (18), MT movement may be impeded by obstacles such as other MTs or unseen cellular components such that the peak rate of movement is only occasionally realized. The distribution of peak movement rates for 15 MTs with bleached marks (Fig. 4) displayed a wide range, from 8.9 μm/min to 40.6 μm/min, perhaps because of the obstruction of MT movement in some cases.

In contrast to the variable velocity for movement of the reference mark, the minus end dynamics relative to the mark were well behaved (Fig. 5*A*). Minus end dynamics were monitored by measuring the distance between the MT minus end and the proximal end of the bleached zone in each frame (Fig. 3). Released minus ends showed variable periods of stability before undergoing a transition to shortening (Fig. 5*A*). The average duration of minus end stability was 1.2 ± 1.3 min. To analyze the rate of shortening of the minus end, we eliminated timepoints in which the minus end was stable and made a histogram of the instantaneous rates during the shortening events (Fig. 5*B*). The average rate of minus end depolymerization was 5.3 ± 3.3 μm/min. Shortening MTs were not observed to revert to the stable state before reaching the bleached mark.

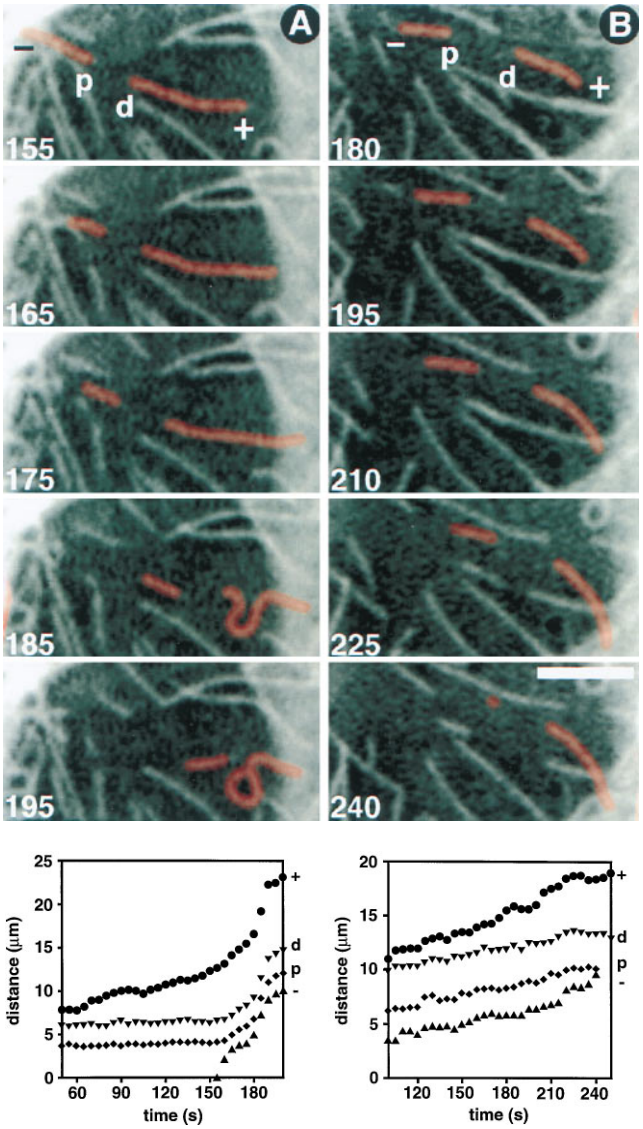

FIG. 3. Marking of MTs by laser bleaching. MTs were marked by a pulse of laser light (514 nm, 480 mW, and 200 ms) producing a 3-μm wide bleached zone. Numbers in the upper left corner of each image correspond to the time (seconds) after bleaching. The minus (−) and plus (+) ends of the MTs, as well as the proximal (p) and distal (d) ends of the bleach zones, are labeled in the first panel of each sequence. Graphs below each sequence show the distance from the centrosome of the MT minus (−, triangles) and plus (+, circles) ends, as well as the proximal (p, diamonds) and distal (d, inverted triangles) ends of the bleached zone vs. time after bleaching. Dotted lines correspond to the times at which the frames were acquired. (*A*) MT was released (155–160 s) and moves away from the centrosome (≥160 s), with the plus end stopping as it reaches the edge of the nuclear–ventral region (185 s). The minus end continues moving (≥185 s), with the MT buckling as a result. (*B*) The MT plus end grows while the minus end shortens (beginning at 215 s), producing treadmilling. This is superimposed on motor-based movement of the MT, as indicated by movement of the bleached bar. The MT was released before laser bleaching was performed. The centrosome is out of the field of view, above the upper left corner. (Bar = 5 μm.)

DISCUSSION

Centrosomal MT Release. In this paper, we report the first, to our knowledge, direct observation of MT release from the centrosome *in vivo*. We do not believe that the observed release was an artifactual result of photodamage to fluorescent MTs because the release rate was not a function of the time of observation and MTs were almost never seen to break. Although our ability to monitor release events varied with the geometry of the cell and the relative congestion of MTs at the centrosome, constitutive release of MTs was seen in all cells examined.

The mechanism for producing MT release is presently unknown. One possible candidate is the MT-severing protein katanin (34). Alternatively, ring complexes (γTuRCs; ref. 35) of γ-tubulin, important for MT nucleation at the centrosome (36), also may possess a release function by promoting detach-

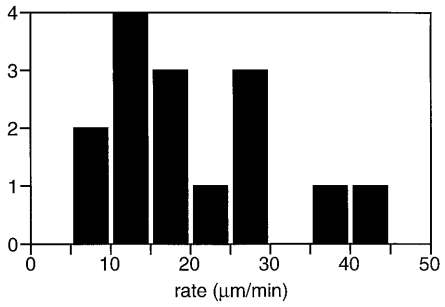

FIG. 4. Distribution of peak rates of translocation of released MTs. Although some released MTs moved at rates >35 μm/min, others reached peak rates of <10 μm/min. The average peak rate was 20.1 μm/min (n = 15).

ment of MTs. An interesting question is whether release occurs between the centrosome and the γTuRC, thus producing a "capped" MT, or between the γTuRC and the MT, thus producing an "uncapped" MT.

MT release from the centrosome may be the primary mechanism for production of noncentrosomal MTs. MT breakage or severing appears to be a very rare event; we observed hundreds of MTs for many hours, and only one MT breakage event was noted. We did occasionally observe the appearance of new fluorescent MT segments in the cytoplasm not visibly connected to the centrosome. These could represent either self-assembly or noncentrosomal nucleation. Alternatively, they could represent growth from the plus ends of preexisting MTs that did not contain labeled tubulin. The frequency of observation of these events was reduced with time after fluorescent tubulin injection as would be expected if they resulted from growth off preexisting ends. However, to rule out self-assembly or noncentrosomal nucleation definitively would require a second MT label allowing visualization of the entire MT.

Movement of Released MTs. MT movement away from the centrosome subsequent to release was found to consist of a combination of translocation and treadmilling of MTs. Translocation could be the result of either a plus end-directed motor associated with the released MT interacting with a parallel MT or a minus end-directed motor associated with an organelle interacting with the released MT. We observed no MT–MT sliding interactions but did observe individual translocating MTs with no closely associated MTs, indicating that the latter possibility is most likely. Movement of MTs in the nuclear–ventral region could be generated by a minus end-directed motor such as cytoplasmic dynein (37) on the nuclear envelope (38), Golgi apparatus, or endoplasmic reticulum (39). However, the transport mechanism does not appear to operate at the cell periphery because no MT movement was evident in that region (ref. 20; unpublished observations).

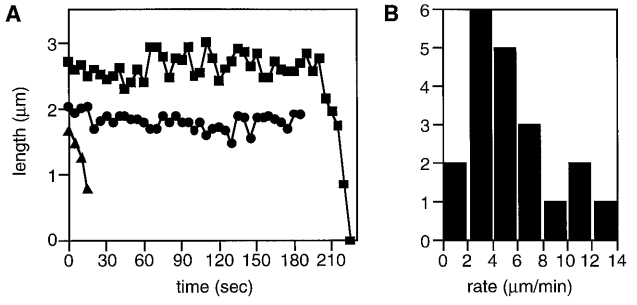

FIG. 5. (*A*) Three examples of the behavior of minus ends of released MTs. One MT (top, squares) was stable during much of the sequence but shortened toward the end. The second MT (middle, circles) was stable during the entire sequence. The third MT (bottom, triangles) was observed to shorten beginning at the time of release. (*B*) Distribution of shortening rates of released MTs. Rates of shortening between pairs of points were determined. The average rate of shortening was 5.3 μm/min (n = 20).

Minus End Dynamics. The observations of release and disassembly of MT minus ends provide a new mechanism for MT turnover. Unlike the dynamic instability observed at plus ends that consists of transitions between phases of growing and shortening, the minus ends were never seen to grow and once having begun to shorten were not observed to return to a stable state. The absence of minus end growth was similar to what has been seen in extracts of porcine brain (40) and frog (41) and sea urchin eggs (42). Minus end growth might be inhibited by a specific factor such as the dimer-binding protein that has been proposed to prevent minus end assembly in sea urchin eggs (43).

In vitro studies using pure tubulin show that MT minus ends grow and shorten but are rarely stable (44), suggesting that the minus end stability we observed was not due to an inherent property of the MTs themselves. Instead, additional protein(s) presumably stabilize the minus ends by coating the MT surface or capping the end. An attractive hypothesis is that the γTuRCs (35) remain attached to the minus ends upon release, thereby blocking disassembly, and become detached after a variable amount of time.

A difference between the minus end depolymerization we observed in interphase cells and that seen for kinetochore MTs in mitotic spindles is that, in the latter case, the MTs depolymerize while remaining attached to the centrosome (27). In contrast, our laser-marking experiments provided no evidence that attached MTs depolymerize at their minus ends in interphase cells.

Role of Release in MT Organization and Turnover. Although there was no obvious organization to MTs in PtK_1 cells under the conditions used here, presumably the mechanism exists nonetheless to generate noncentrosomal MTs should the cells differentiate and develop defined apical and basal surfaces. Instead of proceeding through the MT turnover pathway, the MTs may be stabilized and transported to construct noncentrosomal MT arrays.

An understanding of MT minus end turnover can be formulated in three steps (Fig. 6): release from the centrosome, uncapping of the minus end, and depolymerization. The fraction of the cell's MTs that are noncentrosomal would be dependent on the rate constants for each of the steps. Thus, increasing the rate constant for release or decreasing the rate constants for uncapping or depolymerization would each result in an increased fraction of noncentrosomal MTs. The amount by which minus ends contribute to the total MT turnover depends on the values of the rate constants for each step in the minus end pathway compared with plus end dynamics. Our data for PtK_1 cells provide estimates of the rate constants, allowing a calculation of the half-time for MT turnover

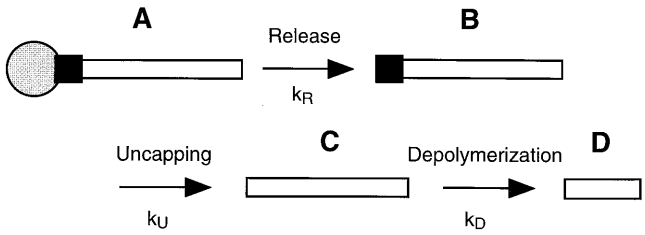

FIG. 6. Minus end turnover pathway. (*A*) MT (open rectangle) attached to the centrosome (shaded circle) with a cap preventing depolymerization at the minus end (filled square). (*B*) MT is released from the centrosome, but the minus end remains capped. (*C*) Cap is stochastic, not permanent; MT has some probability of becoming uncapped. (*D*) MT minus end depolymerizes. k_R, k_U, and k_D are the rate constants for release, uncapping, and depolymerization, respectively.

contributed by the minus end route. Both MT release and uncapping may be modeled as exponential decay processes with half times $t_{[1/2]} = (\ln 2)/k$. The measured rate constant for release (0.06 min^{-1}) yields a $t_{[1/2]}$ of 10.5 min. Based on the average time of minus end stability (1.2 min), the rate constant for uncapping is 0.8 min^{-1}, yielding a $t_{[1/2]}$ of 0.9 min. Assuming an average MT length of 20 μm, the average rate of shortening of 5.3 μm/min gives a $t_{[1/2]}$ for disassembly of 1.9 min. The sum of the three half-times yields a $t_{[1/2]}$ of 13.3 min overall for the minus end turnover pathway. In contrast, as indicated above, analysis of plus end dynamics suggests a much slower turnover process. In particular, from the observed average shortening excursions of MT plus ends (1.6 μm) in PtK_1 cells (22) and an assumed MT length of 20 μm and following a Monte Carlo analysis (24), the estimated $t_{[1/2]}$ for MT turnover would exceed 1 h. In contrast to both minus end (13.3 min) and plus end (>1 h) turnover estimates, the reported $t_{[1/2]}$ for turnover of MTs in PtK_1 cells as determined by photobleaching is on the order of 5 min (23). Although neither mechanism is in quantitative accord with MT turnover data, the minus end pathway is less in discord. The disparity may be even less if our observations of MT transport are taken into account. Although MT transport through the cytoplasm does not contribute to turnover per se, it will appear as turnover in assays using redistribution of fluorescence after photobleaching or photoactivation, leading to faster apparent turnover times. Thus the existence of minus end subunit loss helps to resolve the disparity between highly tempered plus end dynamics observed for individual MTs and rapid polymer exchange results obtained for populations of MTs.

In summary, release, stabilization, and transport of centrosomal MTs may be general mechanisms used by cells to produce noncentrosomal arrays of MTs whereas release and disassembly at the minus end would complement plus end dynamic instability in rapidly altering the MT cytoskeleton. Thus, the relative proportions of centrosomal and noncentrosomal MTs in a cell would result from a steady-state of release, uncapping, and depolymerization. It is interesting to speculate that, for each step of the pathway, there is potential for cellular regulation in response to changes in cell motility or differentiation state.

We thank I. Vorobjev for stimulating discussions in the initial stages of this project. This work was supported by a National Institutes of Health Grant GM25062 to G.G.B. and a National Institutes of Health Postdoctoral Training Grant to T.J.K. Image sequences of data from this paper can be obtained from the Borisy Lab web site at http://borisy.bocklabs.wisc.edu.

1. Cassimeris, L. (1993) *Cell Motil. Cytoskeleton* **26,** 275–281.
2. Bray, D. & Bunge, M. B. (1981) *J. Neurocytol.* **10,** 589–605.
3. Tassin, A.-M., Maro, B. & Bornens, M. (1985) *J. Cell Biol.* **100,** 35–46.
4. Durand-Schneider, A. M., Bouanga, J. C., Feldmann, G. & Maurice, M. (1991) *Eur. J. Cell Biol.* **56,** 260–268.
5. Bré, M.-H., Kreis, T. E. & Karsenti, E. (1987) *J. Cell Biol.* **105,** 1283–1296.
6. Gilbert, T., LeBivic, A., Quaroni, A. & Rodriguez-Boulan, E. (1991) *J. Cell Biol.* **113,** 275–288.
7. Henderson, C. G., Tucker, J. B., Chaplin, M. A., Mackie, J. B., Maidment, S. N., Mogensen, M. M. & Paton, C. C. (1994) *J. Cell Sci.* **107,** 589–600.
8. Bacallao, R., Antony, C., Dotti, C., Karsenti, E., Stelzer, E. H. K. & Simons, K. (1989) *J. Cell Biol.* **109,** 2817–2832.
9. Harris, P., Osborn, M. & Weber, K. (1980) *J. Cell Biol.* **84,** 668–679.
10. Hollenbeck, P. J. & Cande, W. Z. (1985) *Eur. J. Cell Biol.* **37,** 140–148.
11. Kitanishi-Yumura, T. & Fukui, Y. (1987) *Cell Motil. Cytoskeleton* **8,** 106–117.
12. Vorobjev, I. A. & Chentsov, Yu. S. (1983) *Eur. J. Cell Biol.* **30,** 149–153.
13. McBeath, E. & Fujiwara, K. (1990) *Eur. J. Cell Biol.* **52,** 1–16.
14. Meads, T. & Schroer, T. A. (1995) *Cell Motil. Cytoskeleton* **32,** 273–288.
15. Joshi, H. C. & Baas, P. W. (1993) *J. Cell Biol.* **121,** 1191–6.
16. Ahmad, F. J., Joshi, H. C., Centonze, V. E. & Baas, P. W. (1994) *Neuron* **12,** 271–280.
17. Ahmad, F. J. & Baas, P. W. (1995) *J. Cell Sci.* **108,** 2761–2769.
18. Belmont, L. D., Hyman, A. A., Sawin, K. E. & Mitchison, T. J. (1990) *Cell* **62,** 579–589.
19. Mitchison, T. & Kirschner, M. (1984) *Nature (London)* **312,** 237–42.
20. Sammak, P. J. & Borisy, G. G. (1988) *Nature (London)* **332,** 724–726.
21. Schulze, E. & Kirschner, M. (1988) *Nature (London)* **334,** 356–359.
22. Shelden, E. & Wadsworth, P. (1993) *J. Cell Biol.* **120,** 935–945.
23. Saxton, W. M., Stemple, D. L., Leslie, R. J., Salmon, E. D., Zavortink, M. & McIntosh, J. R. (1984) *J. Cell Biol.* **99,** 2175–2186.
24. Gliksman, N. R., Skibbens, R. V. & Salmon, E. D. (1993) *Mol. Biol. Cell* **4,** 1035–1050.
25. Margolis, R. L. & Wilson, L. (1981) *Nature (London)* **293,** 705–711.
26. Rodionov, V. I. & Borisy, G. G. (1997) *Science* **275,** 215–218.
27. Mitchison, T. J. (1989) *J. Cell Biol.* **109,** 637–652.
28. Zhai, Y., Kronebusch, P. J. & Borisy, G. G. (1995) *J. Cell Biol.* **131,** 721–734.
29. Borisy, G. G., Marcum, J. M., Olmsted, J. B., Murphy, D. B. & Johnson, K. A. (1975) *Ann. NY Acad. Sci.* **253,** 107–132.
30. Himes, R. H., Burton, P. R. & Gaito, J. M. (1977) *J. Biol. Chem.* **252,** 6222–6228.
31. Mujundar, R. B., Ernst L. A., Mujundar, S. R., Lewis, C. J. & Waggoner, A. S. (1993) *Bioconjugate Chem.* **4,** 104–111.
32. Mikhailov, A. V. & Gundersen, G. G. (1995) *Cell Motil. Cytoskeleton* **32,** 173–186.
33. Sammak, P. J., Gorbsky, G. J. & Borisy, G. G. (1987) *J. Cell Biol.* **104,** 395–405.
34. McNally, F. & Vale, R. (1993) *Cell* **75,** 419–429.
35. Zheng, Y., Wong, M. L., Alberts, B. & Mitchison, T. (1995) *Nature (London)* **378,** 578–583.
36. Oakley, B. R., Oakley, C. E., Yoon, Y. & Jung, M. K. (1990) *Cell* **61,** 1289–1301.
37. Paschal, B. M., Shpetner, H. S. & Vallee, R. B. (1987) *J. Cell Biol.* **105,** 1273–1282.
38. Murray, A. W., Desai, A. B. & Salmon, E. D. (1996) *Proc. Natl. Acad. Sci. USA* **93,** 12327–12332.
39. Cole, N. B. & Lippincott-Schwartz, J. (1995) *Curr. Opin. Cell Biol.* **7,** 55–64.
40. Allen, C. & Borisy, G. G. (1974) *J. Mol. Biol.* **90,** 381–402.
41. Gard, D. L. & Kirschner, M. W. (1987) *J. Cell Biol.* **105,** 2191–2201.
42. Simon, J. R., Parsons, S. F. & Salmon, E. D. (1992) *Cell Motil. Cytoskeleton* **21,** 1–14.
43. Spittle, C. S. & Cassimeris, L. (1996) *Cell Motil. Cytoskeleton* **34,** 324–335.
44. Walker, R. A., O'Brien, E. T., Pryer, N. K., Soboeiro, M. F., Voter, W. A., Erickson, H. P. & Salmon, E. D. (1988) *J. Cell Biol.* **107,** 1437–1448.